Chemistry and photophysics of mixed cadmium sulfide/mercury sulfide colloids

ARTICLE *in* THE JOURNAL OF PHYSICAL CHEMISTRY · MAY 1993

Impact Factor: 2.78 · DOI: 10.1021/j100122a026

Chemistry and Photophysics of Mixed CdS/HgS Colloids

A. Hässelbarth, A. Eychmüller,* R. Eichberger, M. Giersig, A. Mews, and H. Weller

Abteilung Photochemie, Hahn-Meitner-Institut Berlin GmbH, Glienicker Strasse 100, D-1000 Berlin 39, Germany

Received: October 19, 1992; In Final Form: February 26, 1993

Aqueous co-colloidal systems consisting of two nanocrystalline, size-quantized groups II–VI semiconductor particles were investigated. Coating the HgS colloids with a layer of CdS leads to core–shell-like structures with electronic properties differing considerably to the sum of the separate particles. Implantation of HgS in the surface of CdS gives a new system with very colorful fluorescence properties. Evidence for a charge carrier transfer in this system is obtained from optical spectroscopy. Spectroscopic experiments, as well as electron microscopy studies, give insight into the geometrical and energetic structure and the charge carrier dynamics in such systems.

1. Introduction

Over the past few of years the electronic and luminescence properties of quantum-sized CdS colloids have been the subject of a number of investigations (for reviews, see e.g. refs 1–9). Some interesting phenomena have been described recently and attempts were made to understand them mechanistically. The keywords of these studies are, for example, excitonic, trapped, and delayed fluorescence.[10–14] Beyond that, attention has been drawn to nonlinear optical effects,[15–20] transitions to higher excited states,[21] electron transfer from the conduction band of CdS to quenching molecules[22–30] or from one colloidal particle to others such as AgI,[31] ZnO,[32] Ag_2S,[33] or solid, and colloidal TiO_2.[31,32,34–36] CdS is a very attractive model substance due to its stability, easy preparation and handling, and last, but not least, its distinct band gap that enables one to easily detect a number of optical properties. All the performed experiments underline the importance of the surface condition of the respective CdS particles. This is due to their very small size (2–20 nm) resulting in a large number of molecules being located on the surface, which strongly influences the electronic and consequently the optical properties.[37,38] It is convenient to record the absorption and fluorescence spectra, as well as the time-resolved luminescence behavior of such transparent colloidal solutions to obtain evidence about the charge carrier dynamics and electronic states in size-quantized colloids.

The work we present here was initiated by the question whether or not it is feasible to coat an existing Q-particle by a layer of CdS or to implant a size-quantized semiconductor particle in the surface of a CdS colloid in order to build up more complex hetero structures. Several such systems have previously been described, for example, CdS on ZnS,[39,40] Ag_2S on CdS,[33] Ag_2S on AgI,[41] together with other groups II–VI semiconductor co-colloids such as CdSe–ZnS[42] and CdSe–ZnSe.[43]

Following an earlier brief communication,[44] we report here in detail a new co-colloidal system, namely HgS with CdS. First, we describe experiments with HgS colloids precipitating as cubic β-HgS. HgS was chosen because of its small bandgap in bulk material (0.5 eV). On the HgS seeds, the growth of a layer of CdS was accomplished forming a core–shell structure. The second type of preparation involves CdS ($E_{gap,bulk} = 2.5$ eV) as the starting colloid. As the solubility product of HgS is much smaller than that of CdS, we were able to precipitate HgS on the surface of the CdS colloids. The investigations confirm the high sensitivity of the optical properties of colloidal particles on the chemical nature of their surface.

2. Experimental Section

A. Apparatus. Absorption spectra were measured using a Bruins Instruments Omega 10 spectrophotometer and a Shimadzu MPS 2000 the latter of which allows for the separation of absorption and scattering. Fluorescence spectra were recorded by means of a self-built spectrometer equipped with both a photomultiplier and a germanium detector for UV–vis and near-IR fluorescence, respectively. The spectra were corrected for the characteristics of the excitation lamp, the monochromators, and the detectors.

The excitation source for the time-resolved fluorescence measurements was a frequency-doubled cavity-dumped Rhodamine 6 G dye laser synchronously pumped by an argon ion laser (Models 390, 344, 375, 171 Spectra Physics) producing 6-ps short pulses at a repetition rate selected between 40 and 400 kHz. The decay curves were recorded with a single photon counting system using a Hamamatsu R 2809 microchannelplate photomultiplier allowing an instrumental time resolution of 50 ps.

For electron microscopy, small drops of solution were adsorbed on copper grids coated with carbon support films of 5 nm thickness. The grids were scanned in a Philips CM 12 electron microscope with an acceleration voltage of 120 kV. The microscope was equipped with supertwin objective lenses and an EDAX (X-ray fluorescence) detector.

For imaging, axial illumination was used. All images were made under conditions of minimum phase contrast artifacts[45] with a magnification of 120 000× and 430 000× for high-resolution electron microscopy (HREM).

The best HREM micrographs were digitized with an electronic digitizing camera,[46] supported by an IBM computer. The scan step size was 25.5 μm which was equivalent to 0.061 nm at the sample level. All calculations of the image processing were done on μVax workstations.[47]

Interesting HgS/CdS core–shell particles were extracted in image fields of 128 × 128 pixels or 256 × 256 pixels depending on the cluster size. The aim of image processing was to enhance the periodical information existing in the examined cluster.

B. Preparation of the Colloidal Solutions. CdS on HgS (Core–Shell Particles). A 2-L three-necked round bottom flask with a pH electrode, septum, and gas inlet system for flushing with argon was used. The reactor was filled with 2 L of deionized water containing 2×10^{-4} M sodium polyphosphate (Riedel deHaen, $M = 609$ g/mol) and 1×10^{-5} M $HgCl_2$. After 10 min of flushing with argon, the pH of the solution was adjusted to slightly alkaline (pH = 9.3) with 0.1 M NaOH. Under stirring, 0.45 mL of H_2S was added. After approximately 5 min, the reaction was complete; i.e., the HgS colloidal solution showed no further spectral changes after this period of time. Addition of excess H_2S to an aliquot of this solution yields no absorption changes above 300 nm, indicating that all Hg^{2+} ions have reacted into HgS. To the

0022-3654/93/2097-5333$04.00/0

original solution (without exess H_2S) 2×10^{-4} M $Cd(ClO_4)_2$ and various amounts of H_2S ranging from 1 to 9 mL (2.2×10^{-5} to 2×10^{-4} M) were added.

Smaller HgS particles have been made with 1×10^{-6} M $HgCl_2$ and the stoichiometric amount of H_2S. Precipitation of the 2×10^{-4} M CdS and the addition of 6×10^{-4} M $Cd(ClO_4)_2$ yielded a heterogeneous solution consisting of HgS particles covered with CdS together with pure CdS colloids. Fluorescence quenching experiments were performed using these solutions.

HgS on CdS (Reconstructed CdS Surfaces). The CdS colloid preparation generally followed a method described by Spanhel et al.[37] Since even slight modifications in the preparation conditions affect the size and size distributions of the colloids the exact procedures are outlined below.

The 2×10^{-4} M CdS colloids were prepared following a similar procedure as for precipitating HgS. Using the same flask, a solution of 2 L of deionized water containing 2×10^{-4} M sodium polyphosphate (M = 609 g/mol) and 2×10^{-4} M $Cd(ClO_4)_2$ (Alfa) was brought to pH = 9.3 with 0.1 M NaOH. Under vigorous stirring, 9 mL of H_2S were injected all at once with a syringe into the reactor. The yellow color of CdS developed during the first few minutes. After 10 min the particle growth was stopped by raising the pH with 1 M NaOH to the highly alkaline pH = 12. The addition of 12 mL of 0.1 M $Cd(ClO_4)_2$ gave transparent, colloidal CdS solutions containing no free sulfide ions and showing bright green bandgap luminescence. This preparation results in CdS particles of about 7 nm in diameter (agglomeration number approximately 3500) with fairly narrow size distribution (18% standard deviation)[48] exhibiting cubic crystal structure.[21] From this solution 200 mL was filled into an Erlenmeyer flask and 50 mL of water containing the desired amount of $HgCl_2$ (from 3×10^{-6} to 5×10^{-5} M) was added rapidly under stirring. The emerging co-colloids were ripened for 2 days in the dark at room temperature.

3. Results and Discussion

CdS on HgS (Core–Shell Particles). Figure 1a shows an electron micrograph of pure HgS particles prepared as described in the Experimental Section. Electron diffraction experiments of this sample exhibit the typical parameters of cubic β-HgS. A survey of approximately 300 particles yields the histogram seen in Figure 2 (○). The average diameter of the particles is about 1.8 nm, and the particle size distribution is fairly narrow. Figure 1b shows HgS particles treated with 2×10^{-4} M $Cd(ClO_4)_2$ and 2.2×10^{-5} M H_2S. The corresponding histogram is also depicted in Figure 2 (●). It resembles particles with an average diameter of 2.8 nm and slightly broader size distribution. Thus, we conclude that coated (or core–shell like) HgS/CdS particles were formed by this type of preparation with the HgS particles acting as nucleation seeds during the precipitation of CdS. Probably, the growth of one semiconductor material on the other is favored by the choice of the two materials, since both HgS and CdS have nearly exactly the same lattice constants. If one assumes that the entire amount of CdS grows exclusively on the HgS cores, the mean particle diameter should increase by the third root of the ratio of the molar concentrations after and before the coating, i.e., $(3.2)^{1/3} = 1.47$. A ratio of 1.52 (2.79/1.84 nm) was calculated from the size histograms, which reflects the predicted value very well.

High-resolution micrograph pictures of particles coated in this manner mostly exhibit a dark core with the diameter of the initially used HgS particles surrounded by a light gray shell. In Figure 3a, an individual, relatively large composite particle is shown. The arrows in Figure 3a indicate the direction of the lattice planes. The lattice plane distances typical for HgS and CdS are seen and identified by image processing. The information concerning the cubic structure of both subunits is deduced from power spectra (cf. Figure 3b). In the corresponding EDAX spectrum X-ray

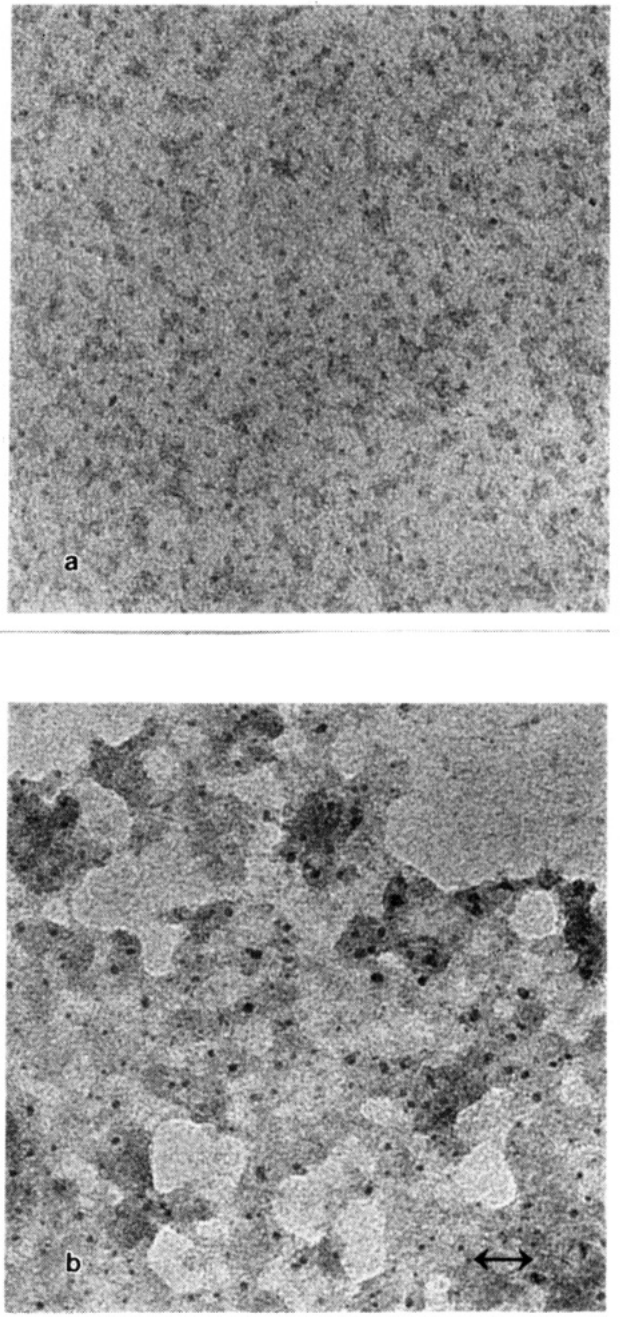

Figure 1. (a, top) Electron micrograph of pure HgS colloids; (b, bottom) core–shell particles, same as (a) but coated with CdS. The bar equals 21 nm.

fluorescence from Cd, Hg and S is present though not exactly in the stoichiometry expected. This particular particle is, in a sense, not typical for the ensemble as most of the composites exhibit unidirectional lattice planes, i.e., an epitaxial growth of the CdS shell on HgS core. The high-resolution micrographs give strong evidence for the core-shell structure in the composite particles and clearly exclude the formation of a mixed binary solid phase of the type $Hg_xCd_{1-x}S$.

The formation of core–shell particles is nicely reflected in the absorption and fluorescence spectra. The unstructured absorption spectrum of pure HgS can be seen in Figure 4, spectrum A. The addition of 2×10^{-4} M $Cd(ClO_4)_2$ yields spectrum B. The absorption decreases slightly over the whole spectral range of absorption. The explanation nearest at hand for this experimental finding is breaking of some HgS bonds to form CdS bonds (and consequently ending up with smaller HgS particles). But this seems to be very unlikely since the solubility product of HgS is more than 20 orders of magnitude smaller than that of CdS. We,

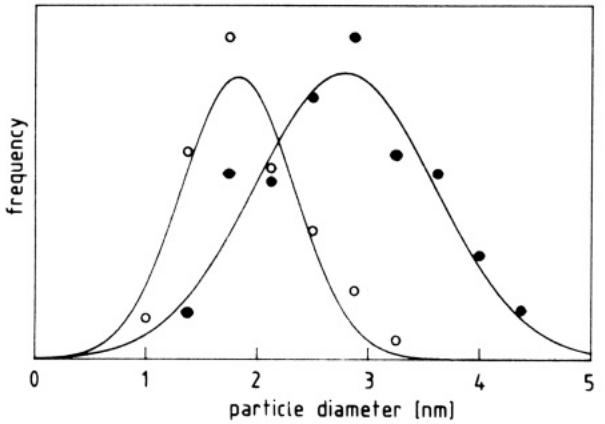

Figure 2. Particle size histograms of HgS (○) and CdS on HgS (●).

therefore, suggest that adsorbed Cd^{2+} ions influence the electronic properties of the HgS particles.

The effect of stepwise addition of portions of 2.2×10^{-5} M H_2S to this solution can be seen in Figure 4, spectra C to H. The absorbance increases in the entire spectral range from spectra B to E, whereas an absorption edge emerges around 480 nm in spectra F to H and no additional increase in the absorbance occurs at longer wavelengths. Scattering as a possible mechanism which might lead to misinterpretation of the long-wavelength absorption has been ruled out: by comparing the spectra taken in "transmission" and "turbidity" mode of our spectrophotometer no differences were detectable, indicating that light scattering due to either larger particles or aggregates of colloids does not occur. In TEM micrographs of sample H, pure CdS particles are seen with diameters of about 6 nm in addition to the composite particles. Thus, we conclude that, up to an addition of about 7×10^{-5} M CdS to the original HgS sol, mainly coated particles and at higher concentrations additional separate CdS particles are formed. The absorption spectra of the coated particles (up to sample E in Figure 4) do not reflect a superposition of HgS and CdS spectra. It appears as if by coating with CdS the absorbance of the HgS core is enhanced. The maximum amount of CdS which is precipitated in the form of a shell on the HgS core corresponds to approximately 2 monolayers.

Figure 5 shows the fluoroscence spectra (λ_{exc} = 360 nm) corresponding to the absorption spectra shown in Figure 4. Solutions A and B (pure HgS and HgS with Cd^{2+} ions) do not fluoresce at all. A strong fluorescence band with a maximum at 950 nm occurs after the first addition of H_2S (the slight dent in the HgS fluorescence band is due to absorption of the solvent water). Increasing amounts of H_2S do not change its spectral position. The intensity, however, increases until approximately 7×10^{-5} M H_2S is added, which is nearly the same amount of additive after which the absorption at $\lambda > 500$ nm also no longer increases on addition of more H_2S. Obviously, we have generated fluorescence in the HgS particles by covering them with CdS, whereas the separately formed CdS particles do not contribute to the fluorescence.

A fluorescence "activation" of this kind was also observed in the systems $Cd(OH)_2$ on CdS[37] and ZnS on CdSe.[42] Following the arguments given in these references the fluorescence activation is interpreted as the removal of traps for nonradiative recombinations, mainly by a coordinative saturation of surface anions. Due to the shape and the spectral position one could ascribe the observed fluorescence to the recombination of trapped charge carriers at the interface of the HgS core and the CdS shell. The fluorescence could just as well arise from band to band recombination in the HgS core. In this case the width of the fluorescence band would reflect the size distribution of the HgS cores. As demonstrated in ref 14, temperature-dependent fluorescence experiments should help to clarify the location of where the charge carriers recombine.

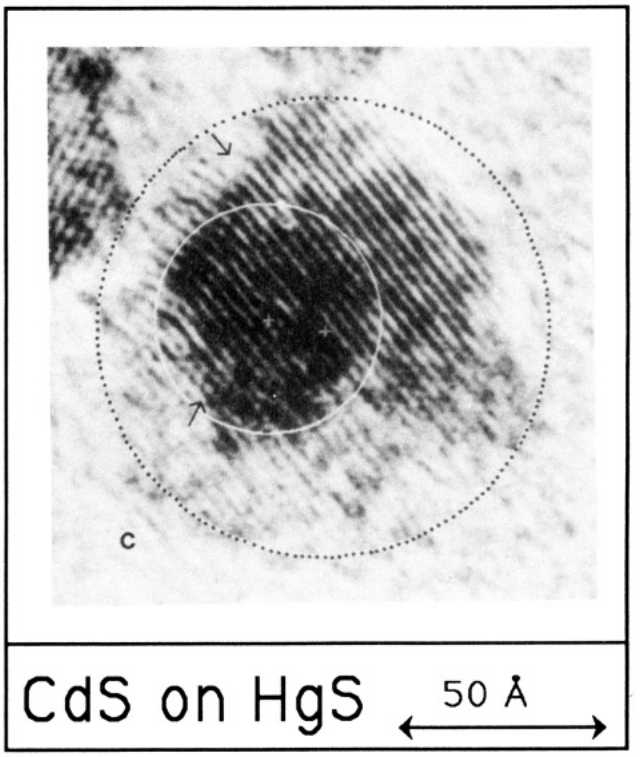

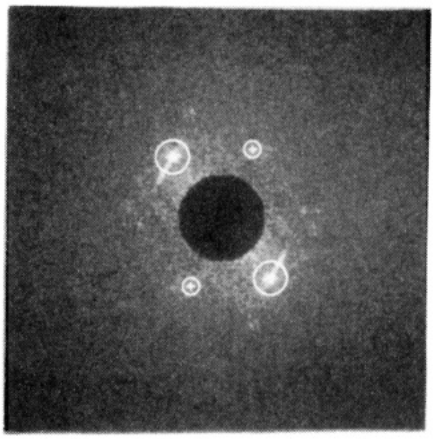

Figure 3. (a, top) High-resolution electron micrograph of a single particle from Figure 1b. The arrows indicate the directions of the lattice planes of the core (HgS) and the shell (CdS). (b, bottom) Power spectrum of (a) showing the typical reflexes of cubic CdS (big circles) of 1/3.3 $Å^{-1}$ and cubic β-HgS (small circles) of 1/3.3 $Å^{-1}$.

The evidence for the formation of a core–shell structure instead of a mixed solid phase is also supported by the fluorescence properties. Namely, if a $Hg_xCd_{1-x}S$ phase would be formed during the growth of CdS on HgS, the molar ratio of Hg and Cd should decrease and, as a consequence, the fluorescence band should shift spectrally. On the contrary, it was found that the spectral position of the fluorescence remains fixed with increasing amount of deposited CdS and that only the intensity of the luminescence increases concomitantly. As outlined above, the latter is understood as a gradual removal of nonradiative recombination centers during the formation of a compact CdS layer on the surface of the HgS core.

As a further proof for the spectral assignments excess Cd^{2+} ions (6×10^{-4} M) were added at pH 11 to sample H; i.e., the sample in which a CdS absorption is seen as well as the absorbance of the core–shell particles. This is a well-established procedure to activate the fluorescence of separately formed, phosphate stabilized CdS particles.[37] The fluorescence spectra of sample H before and after this activation procedure are shown in Figure 6. It is recognized that the fluorescence at long wavelengths

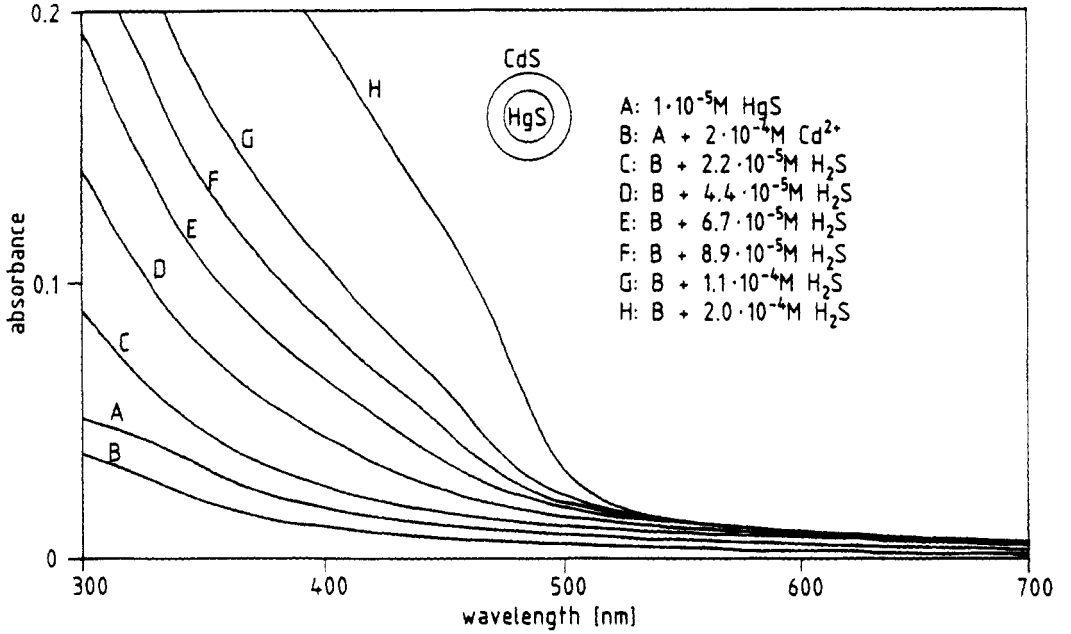

Figure 4. Absorption spectra of core–shell particles CdS on HgS. Spectrum A, pure HgS; spectrum B, A after the addition of 2×10^{-4} M Cd^{2+}; spectra C–H, B after the addition of various amounts of H_2S as indicated.

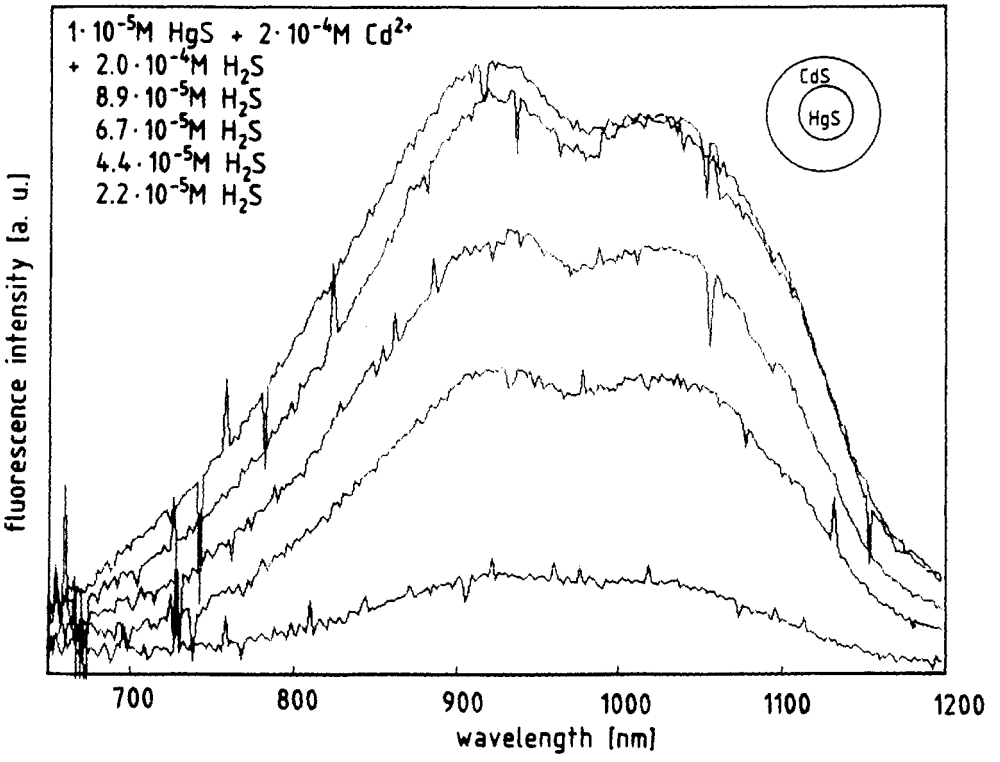

Figure 5. Fluorescence spectra of core–shell particles CdS on HgS (λ_{exc} = 360 nm).

remains unchanged and that two new fluorescence bands appear at shorter wavelengths. The difference between the two spectra gives the well-known fluorescence spectrum of pure activated 6-nm CdS particles. In the inset of the figure two excitation spectra of the activated sample H are plotted, one recorded at the observation wavelength of 650 nm and the other at 1100 nm, respectively (arrows in Figure 6). It can be seen clearly that the excitation spectrum recorded at 1100 nm, i.e., a spectral region in which CdS does not fluoresce, shows no CdS absorption edge but resembles the unstructured absorption spectrum of HgS/CdS core–shell particles. The absorption edge of CdS can be seen clearly, however, when observing the fluorescence at 650 nm, a wavelength at which both HgS and CdS emit. This is clear evidence that two types of particles are present in sample H which fluoresce independently from one another.

Very similar spectral features, as shown in Figures 4, 5, and 6, were observed when somewhat smaller HgS particles were used in the starting sol prior to the CdS coating procedure (cf. Experimental Section). In this case the resulting fluorescence band has a maximum at 800 nm, i.e., 200 nm shifted to shorter wavelengths, a phenomenon understood in terms of size quantization of the HgS core. It was found that in the subsequently activated sample (as in Figure 6) only CdS fluorescence could be quenched with methylviologen, whereas the fluorescence of the composite particles was not quenchable. This may be yet another hint for the core–shell like structure generated: the MV^{2+} does not come into contact with the HgS core in the composite particles due to the shielding of the core by CdS. This conclusion concerning the geometrical structure is in contrast to the results obtained with the reversely prepared particles, i.e., HgS on CdS.

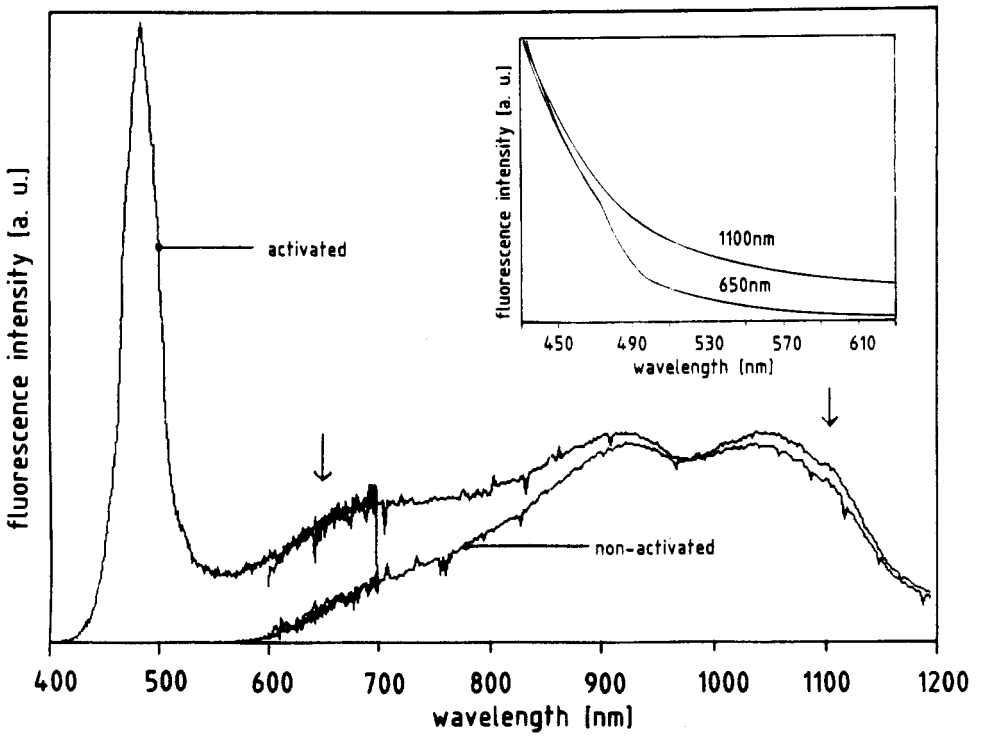

Figure 6. Fluorescence spectrum of sample H (nonactivated) and after the addition of 2×10^{-4} M Cd^{2+} (activated). Inset: fluorescence excitation spectra obtained at 650 and 1100 nm.

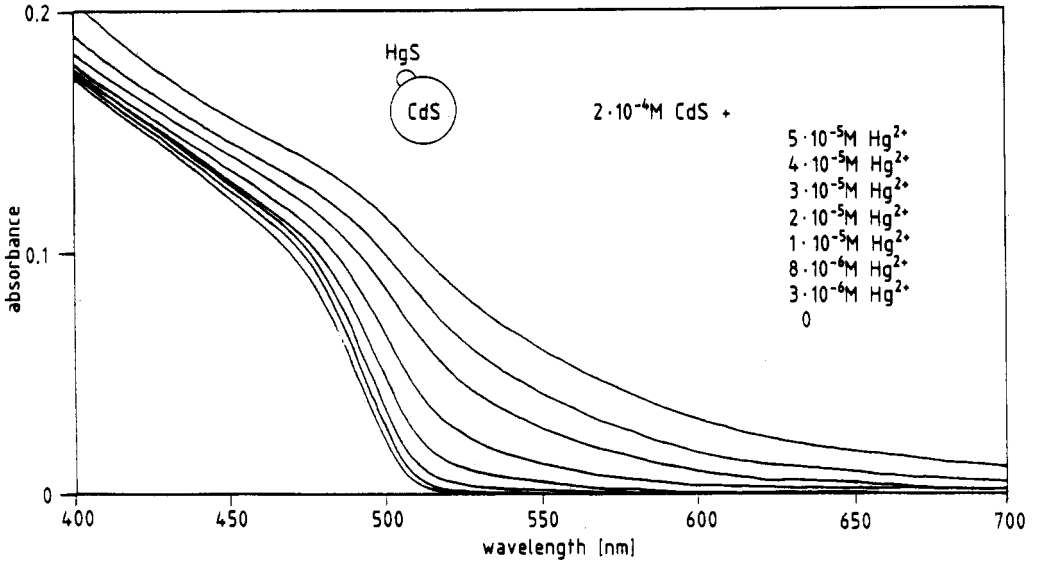

Figure 7. Absorption spectra of composite particles HgS on CdS. Pure CdS (lowest spectrum) and after the addition of various amounts of $HgCl_2$ as indicated.

In these structures the HgS part is exposed to the solution and, consequently, its fluorescence is also quenchable (see below).

HgS on CdS. In the remainder of this article experiments with HgS precipitated on the surface of CdS particles will be discussed.

Figure 7 shows a set of absorption spectra of colloidal CdS with different amounts of added $HgCl_2$. The absorption edge of colloidal size-quantized CdS is clearly seen at about 480 nm. With increasing amounts of added $HgCl_2$ the onset of absorption shifts to longer wavelengths reaching the red and finally infrared spectral region. This absorption behavior is attributed to the formation of size-quantized HgS. The more $HgCl_2$ is added, the larger the HgS particles are and the smaller the bandgap becomes. Due to the much lower solubility of HgS compared with CdS, the addition of $HgCl_2$ to CdS particles results in an exchange of Cd^{2+} by Hg^{2+} (eq 1). Similar to the situation of the core–shell

$$(CdS)_n + mHgCl_2 \rightarrow (CdS)_{n-m}(HgS)_m + mCdCl_2 \quad (1)$$

HgS/CdS particles, the absorption spectra of the attached composite CdS–HgS particles are not simply superpositions of the two size-quantized semiconductors as is easily seen in the uppermost spectrum in Figure 7. Although only 25% of the CdS is converted to HgS, there is only a hint of the CdS absorption edge in this spectrum. Thus, we conclude that the electronic structure of the CdS particles is strongly influenced by surface-bound HgS. As the amount of $HgCl_2$ used in our experiments was much less than that required to cover each CdS particle with a complete monolayer, the formation of a core–shell structure can be excluded.

Besides the hint that no intercalation of mercury ions into cadmium sulfide was observed in the experiments with the core–shell particles, the formation of an isotropic mixed crystal $Cd_xHg_{1-x}S$ can be excluded as a consequence of the fluorescence lifetime measurements together with the fluorescence excitation spectra outlined below. They clearly show that the particles

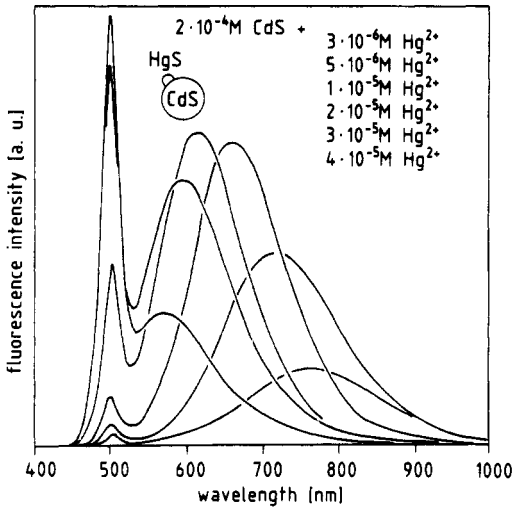

Figure 8. Fluorescence spectra of composite particles HgS on CdS (λ_{exc} = 360 nm).

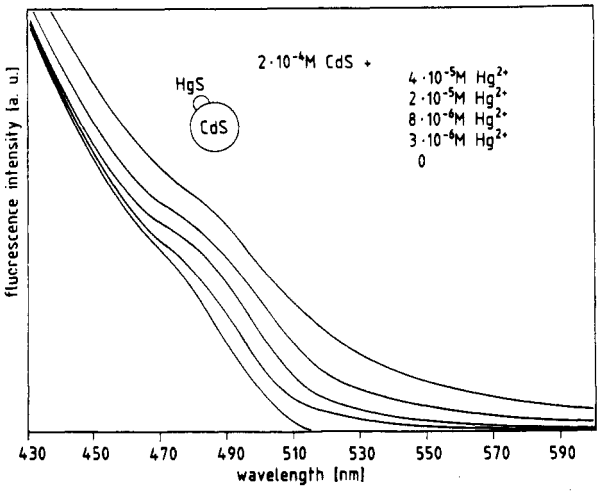

Figure 9. Fluorescence excitation spectra of composite particles HgS on CdS with differently sized HgS parts (λ_{obs} = 650 nm).

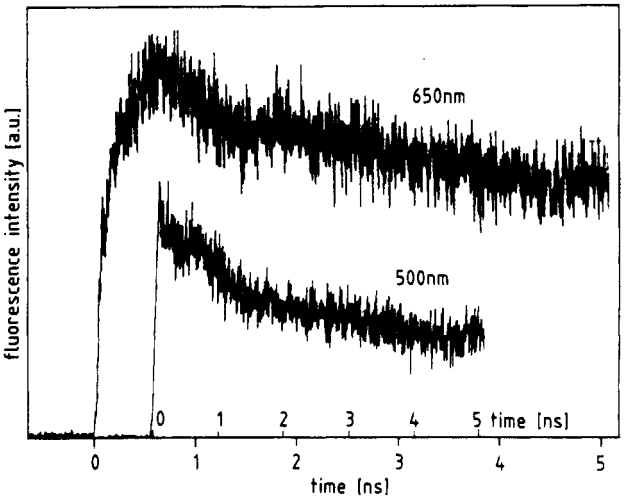

Figure 10. Time-resolved fluorescence of pure CdS (λ_{obs} = 500 nm) and HgS on CdS (λ_{obs} = 650 nm). Excitation wavelength λ_{exc} = 300 nm.

exhibit local differences in composition which justify the use of a pictogram like the one shown in Figure 7. However, in the very early stages of the growth of HgS on CdS one faces a situation which may be described as a locally mixed crystal. In such nanoheterogeneous systems, this raises the interesting question of how many HgS molecules have to be linked among themselves in an environment of CdS to justify the name "HgS particle on CdS". In the context of this work this more or less philosophical question is not answered.

Figure 8 shows a set of fluorescence spectra of colloidal CdS solutions with different amounts of added $HgCl_2$ as indicated. As reported in our earlier communiation,[44] the intense green excitonic fluorescence of CdS at about 500 nm is effectively quenched and luminescence bands develop at longer wavelengths with maxima ranging between 550 and 770 nm depending on the amount of $HgCl_2$ added. This luminescence is attributed to the fluorescence of size-quantized HgS particles formed on the surface of the CdS particles. A fluorescence arising from the radiative recombination of one carrier remaining in the CdS part and the other being transferred into the HgS moiety seems to be unlikely since this long-wavelength fluorescence is obtained also after direct excitation of the HgS moiety with $\lambda_{exc} > 500$ nm. The fluorescence intensity of the particles slowly increases after mixing the CdS and $HgCl_2$. After 2 days at room temperature, there is no further change for at least months. The induction period of 2 days may indicate a slow annealing of defects on the surface of the HgS particles, which are assumed to act as centers for radiationless recombination. Heating accelerates the annealing process.

Fluorescence excitation spectra were recorded with a series of CdS colloids containing different amounts of HgS. An observation wavelength of 650 nm was chosen in order to obtain information about the origin of the long-wavelength luminescence (Figure 9). A comparison of these spectra with the respective set of absorption spectra shows that the main characteristics are identical, i.e., the CdS absorption edge at 480 nm, the long-wavelength absorption of HgS, and its shift to longer wavelengths with increasing particle size. (The slight differences are due to apparative characteristics.) From these experiments, the formation of a significant fraction of separately formed HgS particles can be excluded. Thus, we propose that, according to eq 1, composite particles consisting of a 7-nm CdS component and tiny HgS seeds at the surface are formed. Structures of this kind were also proposed following measurements with CdS–Ag_2S[33] and AgI–Ag_2S.[41]

In Figure 10 two fluorescence decay curves (λ_{exc} = 300 nm) with the co-colloidal structures in the nanosecond range are depicted. The decay kinetics of pure CdS fluorescence recorded at 500 nm have been reported earlier by several authors.[10-14] This behavior is well understood in terms of the recombination of electron–hole pairs in nanocrystals involving shallow electron traps giving rise to delayed fluorescence. In Figure 10 one recognizes an instantaneous appearance of the CdS fluorescence (500 nm) whereas a certain rise time (about 200 ps) of the HgS fluorescence recorded at 650 nm is observed. The buildup of the HgS fluorescence is attributed to charge carrier transfer from the CdS (which absorbs most strongly at the excitation wavelength of 300 nm) to the HgS moiety of the particles.

In Figure 11 a set of fluorescence decay curves recorded at 500 nm is plotted. The uppermost decay curve is recorded with a sample of pure CdS colloid and the other two with different amounts of added $HgCl_2$ as indicated in the figure. It is seen that the decay *kinetics* remain unchanged compared to the excitonic fluorescene of pure CdS irrespective of the quantity of added $HgCl_2$ whereas the *initial height* (or intensity) decreases with increasing HgS content. In Figure 12 we plotted the inital height of the CdS fluorescence from the time resolved experiments as a function of the Hg^{2+} concentration (○). The integral fluorescence intensities of the excitonic CdS fluorescence derived from stationary experiments are shown together with these data (●). Both intensities exhibit the same concentration dependence.

Three energy diagrams suitable for explaining the experimental spectroscopic findings are depicted in Figure 13. The scheme labeled 1 represents pure CdS colloids which behave as described previously.[12-14] That is, after light absorption the photogenerated electrons are quickly trapped in shallow traps on the surface of the particles from where they might be detrapped into the

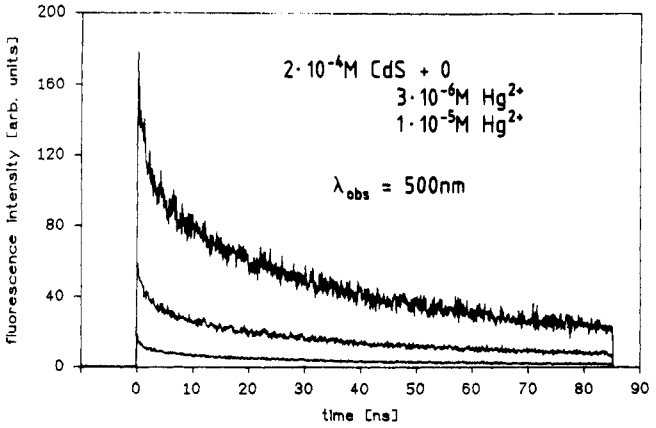

Figure 11. Decay of the excitonic fluorescence of pure CdS (top) and after the addition of $HgCl_2$ as indicated (λ_{exc} = 300 nm, λ_{obs} = 500 nm).

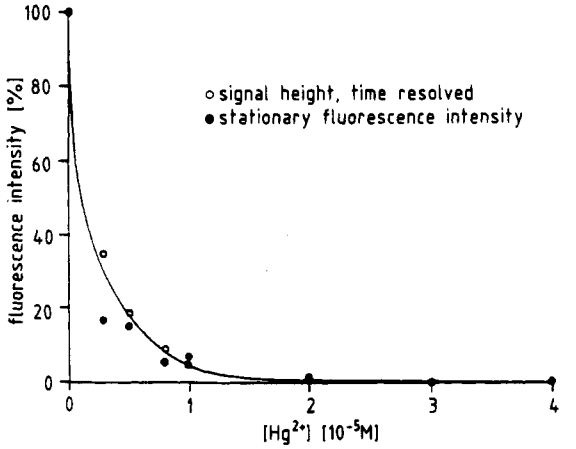

Figure 12. Initial signal height from time resolved measurements (O) and integral fluorescence intensity (●) of the excitonic CdS fluorescence as a function of the Hg^{2+} concentration.

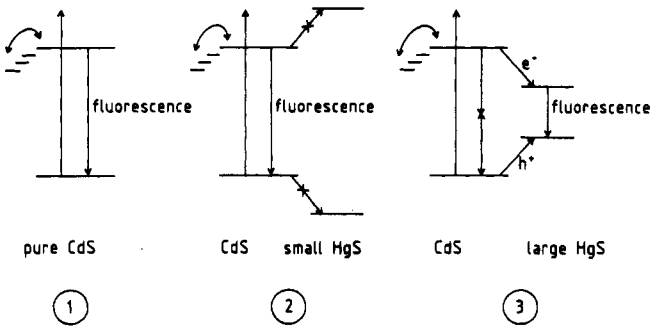

Figure 13. Energy schemes illustrating the photophysical processes taking place in pure CdS (1), CdS with small (2), and larger (3) HgS attached.

conduction band giving rise to the delayed excitonic fluorescence of CdS nanocrystals. This mechanism does not change significantly when the HgS formed is small enough to exhibit an energetic situation like the one shown in picture 2. Neither the electrons from the conduction band nor the holes from the valence band of CdS are transferred to the HgS moiety, and the fluorescence of the CdS remains unchanged. As the HgS particles grow by the addition of $HgCl_2$, more and more co-colloids reach the situation labeled 3 in Figure 13. In these structures hole transfer from the CdS to the HgS valence band is assumed to be much faster than the fluorescence in the CdS moiety. As a result, these particles do not show any CdS fluorescence at all. Considering our time resolution of about 50 ps, the hole transfer must be faster than $2 \times 10^{10}\ s^{-1}$, which is not unreasonable bearing in mind the similarity of the bulk band structures of the CdS and HgS valence bands. After hole capture from the CdS, the electron is eventually transferred to the HgS part where radiative electron–

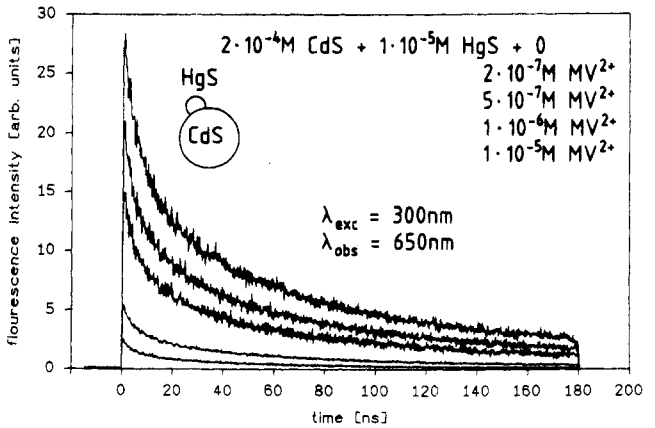

Figure 14. Decay curves of the HgS fluorescence (λ_{exc} = 300 nm, λ_{obs} = 650 nm) in HgS on CdS composites with methylviologen as electron scavenger.

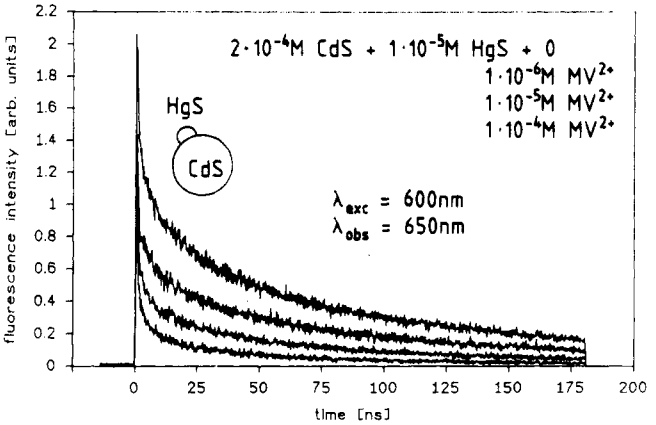

Figure 15. Same as Figure 14 but λ_{exc} = 600 nm.

hole recombination can occur. Thus, in a certain sense, the solutions prepared are inhomogeneous. Even if the assumption holds that all the CdS particles carry the same number of HgS *molecules* (an assumption which does not have to be valid since the mixing process may introduce inhomogeneities by itself), the sizes of the HgS *particles* may vary from co-colloid to co-colloid. Some may carry a larger number of very small HgS particles leading to an energetic situation like the one shown as 2 in Figure 13. Others carry a smaller number of larger HgS particles and so have a more type 3 character.

Fluorescence quenching experiments were carried out using a CdS colloid with 1×10^{-5} M HgS on its surface and methylviologen as the electron scavenger. In the fluorescence decay curves observed at 500 nm, it is seen that the decay becomes faster with increasing quencher concentration, whereas the initial height of the signals is unaffected. This behavior is often called dynamic quenching, meaning that quenching is a process competing with the radiative recombination of the charge carriers. The HgS luminescence, however, behaves differently. The signal height decreases with increasing amounts of added MV^{2+} and, additionally, the decay becomes slightly faster (cf. Figure 14).

In Figure 15 we plotted a number of luminescence decay curves obtained after excitation of the CdS/HgS co-colloids at 600 nm. From these curves it is seen that the signal height remains unchanged, but that the luminescence decay is accelerated with increasing MV^{2+} concentration.

Together, these fluorescence quenching experiments indicate that the electron transfer to the quencher mainly occurs out of the CdS part of the composite particle if excitation is in the UV. It has recently been shown that electron transfer from CdS particles to acceptor molecules occurs out of shallow surface traps.[49] We, therefore, assume that also in the case of CdS/HgS composite particles shallow electron traps are involved in the

fluorescence quenching reactions described here. This mechanism implies that the major effect of methylviologen on the decay curves of the HgS fluorescence (Figure 14) is to decrease the initial signal height as the electrons are scavenged before they reach the HgS. In addition to this reaction, electron transfer can also occur from the tiny HgS deposits. This is seen in the acceleration of the fluorescence decay after the direct excitation of the HgS deposits (Figure 15). The fluorescence quenching experiments support our conclusion that the buildup of the HgS fluorescence lasting 200 ps after excitation of the CdS part is due to a relatively slow electron transfer and not to a transfer of the hole. If, namely, the electron transfer would occur extremely rapidly, the electrons would not be available for methylviologen before they reach the HgS deposits.

4. Final Remarks

Different types of composite CdS–HgS particles can be synthesized on the base of colloid chemistry. The powerful combination of stationary and time-resolved optical spectroscopy with electron microscopy allows detailed structural information about these systems to be obtained.

The composite particles exhibit a series of novel electronic properties which will be subject of further investigations, e.g., in the field of nonlinear optics. As has been outlined, the electronic properties of neither the core–shell type nor the HgS on CdS particles are simple superpositions of the electronic properties of the separate nanocrystals. We propose that the photogenerated exciton in such a composite particle cannot be strictly confined in the HgS core or CdS shell but feels a potential which is formed by the entire composite particle. Similar conclusions have been drawn by the authors of ref 42 who in addition to preparative work numerically modeled the system CdSe on ZnS.

If one keeps in mind that the bulk exciton diameter in CdS and HgS is larger than the diameter of the whole composite particle, such a mixing of the electronic levels of core and shell becomes feasible. This explanation is somewhat similar to the state mixing of the valence band and surface traps in Q-CdSe proposed by Bawendi et al.[50] In this context it is interesting to refer to recent experiments with Q-CdS particles in which a postpreparative exchange of the solvent or the stabilizer[38] influences only the fluorescence properties but not the optical absorption of the particles. It was concluded that the electronic structure of the core was not influenced significantly by the applied surface modification and/or change in environment. The major difference between the examples described in ref 38 and the HgS–CdS composites is that in the latter case the added species becomes part of the crystalline structure by being covalently bound. Stabilizers and solvent molecules are only coordinatively bound to the surface. Obviously, a surface modification of this kind only influences the more or less localized trap states, which determine the fluorescence properties but not the absorption properties.

One might expect that surface traps of a semiconductor core can be eliminated by coating with a wide-bandgap material. This should lead to an enhancement of the excitonic transition of the core. Such an effect, however, is not observable in our system presented here, most probably since the spectra of the HgS particles used for these experiments are unstructured as a consequence of the particle size distribution together with the strong confinement of the charge carriers.

The next step in the nanostructuration of Q-particles will be the formation of three-layered particles which might be considered as nanometer-sized spherical quantum wells. First indications for structures of this kind have already been found in our laboratory. We will report on these experiments in a forthcoming paper.

Acknowledgment. Thanks are due to Lynne Katsikas and Dr. Ivanka Popovic for carefully reading the manuscript.

References and Notes

(1) Henglein, A. *Pure Appl. Chem.* **1984**, *56*, 1215.
(2) Brus, L. E. *IEEE J. Quantum Electron.* **1986**, *22*, 1909.
(3) Brus, L. E. *J. Phys. Chem.* **1986**, *86*, 2555.
(4) Henglein, A. *Top. Curr. Chem.* **1988**, *143*, 115.
(5) Henglein, A. *Chem. Rev.* **1989**, *89*, 1861.
(6) Wang, Y.; Herron, N. *J. Phys. Chem.* **1991**, *95*, 525.
(7) Weller, H. *Angew. Chem.* **1993**, *105*, 43; *Angew. Chem., Int. Ed.* **1993**, *32*, 41.
(8) Weller, H. *Adv. Mater.* **1993**, *5*, 88.
(9) Weller, H.; Eychmüller, A.; Vogel, R.; Katsikas, L.; Hässelbarth, A.; Giersig, M. *Isr. J. Chem.*, in press.
(10) Chestnoy, N.; Harris, T. D.; Hull, R.; Brus, L. E. *J. Phys. Chem.* **1986**, *90*, 3393.
(11) Wang, Y.; Herron, N. *J. Phys. Chem.* **1988**, *92*, 4988.
(12) O'Neil, M.; Marohn, J.; McLendon, G. *J. Phys. Chem.* **1990**, *94*, 4356.
(13) Eychmüller, A.; Hässelbarth, A.; Katsikas, L.; Weller, H. *J. Lumin.* **1991**, *48 & 49*, 745.
(14) Eychmüller, A.; Hässelbarth, A.; Katsikas, L.; Weller, H. *Ber. Bunsenges. Phys. Chem.* **1991**, *95*, 79.
(15) Haase, M.; Weller, H.; Henglein, A. *J. Phys. Chem.* **1988**, *92*, 4706.
(16) Hilinski, E. F.; Lucas, P. A.; Wang, Y. *J. Chem. Phys.* **1988**, *89*, 3435.
(17) Kamat, P. V.; Dimitrijevic, N. M.; Nozik, A. J. *J. Phys. Chem.* **1989**, *93*, 2873.
(18) Wang, Y.; Herron, N.; Mahler, W.; Suna, A. *J. Opt. Soc. Am.* **1989**, *B6*, 808.
(19) Kaschke, M.; Ernsting, N. P.; Müller, U.; Weller, H. *Chem. Phys. Lett.* **1990**, *168*, 543.
(20) Rajh, T.; Micic, O. I.; Lawless, D.; Serpone, N. *J. Phys. Chem.* **1992**, *96*, 4633.
(21) Katsikas, L.; Eychmüller, A.; Giersig, M.; Weller, H. *Chem. Phys. Lett.* **1990**, *172*, 201.
(22) Ramsden, J. J.; Grätzel, M. *J. Chem. Soc., Faraday Trans. 1* **1984**, *80*, 919.
(23) Nosaka, Y.; Fox, M. A. *J. Phys. Chem.* **1986**, *90*, 6521.
(24) Lee, Y. F.; Olshavsky, M.; Chrysochoos, J. *J. Less-Common Met.* **1989**, *148*, 259.
(25) Mills, A.; Douglas, P.; Williams, G. *J. Photochem. Photobiol. A: Chem.* **1989**, *48*, 397.
(26) Kamat, P. V.; Ebbesen, T. W.; Dimitrijevic, N. M. *Chem. Phys. Lett.* **1989**, *157*, 384.
(27) Shiragami, T.; Pac, C.; Yanagida, S. *J. Phys. Chem.* **1990**, *94*, 504.
(28) Nosaka, Y.; Ohta, N.; Miyama, H. *J. Phys. Chem.* **1990**, *94*, 3752.
(29) Chrysochoos, J. *J. Lumin.* **1991**, *48 & 49*, 709.
(30) Rajh, T.; Rabani, J. *Langmuir* **1991**, *7*, 2054.
(31) Gopidas, K. R.; Bohorquez, M.; Kamat, P. V. *J. Phys. Chem.* **1990**, *94*, 6435.
(32) Spanhel, L.; Weller, H.; Henglein, A. *J. Am. Chem. Soc.* **1987**, *109*, 6632.
(33) Spanhel, L.; Weller, H.; Fojtik, A.; Henglein, A. *Ber. Bunsenges. Phys. Chem.* **1987**, *91*, 88.
(34) Gerischer, H.; Lübke, M. *J. Electroanal. Chem.* **1986**, *204*, 225.
(35) Vogel, R.; Pohl, K.; Weller, H. *Chem. Phys. Lett.* **1990**, *174*, 241.
(36) Kiezmann, R.; Willig, F.; Weller, H.; Vogel, R.; Nath, D. N.; Eichberger, R.; Liskas, P.; Lehnert, J. *Mol. Cryst. Liq. Cryst.* **1991**, *195*, 169.
(37) Spanhel, L.; Haase, M.; Weller, H.; Henglein, A. *J. Am. Chem. Soc.* **1987**, *109*, 5649.
(38) Resch, U.; Eychmüller, A.; Haase, M.; Weller, H. *Langmuir* **1992**, *8*, 2215.
(39) Weller, H.; Koch, U.; Gutiérrez, M.; Henglein, A. *Ber. Bunsenges. Phys. Chem.* **1984**, *88*, 649.
(40) Youn, H. C.; Baral, S.; Fendler, J. H. *J. Phys. Chem.* **1988**, *92*, 6320.
(41) Henglein, A.; Gutiérrez, M.; Weller, H.; Fojtik, A.; Jirkovsky, J. *Ber. Bunsenges. Phys. Chem.* **1989**, *93*, 593.
(42) Kortan, A. R.; Hull, R.; Opila, R. L.; Bawendi, M. G.; Steigerwald, M. L.; Carroll, P. J.; Brus, L. E. *J. Am. Chem. Soc.* **1990**, *112*, 1327.
(43) Hoener, C. F.; Allan, K. A.; Bard, A. J.; Campion, A.; Fox, M. A.; Mallouk, T. E.; Webber, S. E.; White, J. M. *J. Phys. Chem.* **1992**, *96*, 3812.
(44) Eychmüller, A.; Hässelbarth, A.; Weller, H. *J. Lumin.* **1992**, *53*, 113.
(45) Kunath, W.; Zemlin, F.; Weiss, K. *Ultramicroscopy* **1985**, *16*, 123.
(46) DATACOPY Model 610 F, Data Copy Corp., Long Beach, CA.
(47) Software used: IMAGIC-V, Image Science GmbH, Berlin, FRG.
(48) Eychmüller, A.; Katsikas, L.; Weller, H. *Langmuir* **1990**, *6*, 1605.
(49) Hässelbarth, A.; Eychmüller, A.; Weller, H. *Chem. Phys. Lett.* **1993**, *203*, 271.
(50) Bawendi, M. G.; Carroll, P. J.; Wilson, W. L.; Brus, L. E. *J. Chem. Phys.* **1992**, *96*, 946.